

OPEN

First Clinical Experience With [⁶⁸Ga]Ga-FAPI-46-PET/CT Versus [¹⁸F]F-FDG PET/CT for Nodal Staging in Cervical Cancer

Simone Wegen, MD,* Katrin Sabine Roth, MD,† Jasmin Weindler, MD,† Karina Claus, MD,* Philipp Linde, MD,* Maike Trommer, MD,* Dennis Akuamo-Boateng, MD,* Lutz van Heek, MD,† Christian Baues, MD,* Birgid Schömig-Markiefka, MD,‡ Klaus Schomäcker, PhD,† Thomas Fischer, PhD,† Alexander Drzezga, MD,†§|| Carsten Kobe, MD,† Christhardt Köhler, MD,¶ and Simone Marnitz, MD*

Introduction: In several solid tumors, fibroblast activation protein (FAP) is overexpressed by cancer-associated fibroblasts in the tumor microenvironment. Preliminary evidence suggests that detection and staging are feasible with PET/CT imaging using [⁶⁸Ga]-radiolabeled inhibitors of FAP also in cervical cancer (CC). Our study aims to explore the accuracy of [⁶⁸Ga]Ga-fibroblast activation protein inhibitor (FAPI)-46 PET/CT and [¹⁸F]F-FDG PET/CT compared with histopathological results of surgical lymph node (LN) staging before primary chemoradiation.

Methods: Seven consecutive women with treatment-naïve and biopsy-proven locally advanced CC underwent both whole-body [⁶⁸Ga]Ga-FAPI-46- and [¹⁸F]F-FDG PET/CT, for imaging nodal staging before systematic laparoscopic lymphadenectomy of the pelvic and para-aortic region. Location and number of suspicious LNs in PET imaging were recorded and compared with the results of histopathological analysis, including immunohistochemical staining for FAP.

Results: All 7 patients had focal uptake above background in their tumor lesions in [⁶⁸Ga]Ga-FAPI-46 PET/CT. [⁶⁸Ga]Ga-FAPI-46 PET/CT showed a higher tumor-to-background ratio (TBR) in primary tumor as well as in LN metastasis. Median TBR_{max} values using liver were 32.02 and 5.15 for [⁶⁸Ga]Ga-FAPI-46 PET/CT and [¹⁸F]F-FDG PET/CT, respectively. Median TBR_{max} using blood pool was 18.45 versus 6.85 for [⁶⁸Ga]Ga-FAPI-46 PET/CT and [¹⁸F]F-FDG PET/CT, respectively. Higher TBR also applies for nodal metastasis: TBR_{max} was 14.55 versus 1.39 (liver) and 7.97 versus 1.8 (blood pool) for [⁶⁸Ga]Ga-FAPI-46 PET/CT and [¹⁸F]F-FDG PET/CT, respectively. Overall, [⁶⁸Ga]Ga-FAPI-46 PET/CT detected more lesions compared with [¹⁸F]F-FDG PET/CT. Following surgical staging, a total of 5 metastatic LNs could be pathologically confirmed, of which 2 and 4 were positive by [¹⁸F]F-FDG PET/CT and [⁶⁸Ga]Ga-FAPI-46 PET/CT, respectively.

Conclusion: [⁶⁸Ga]Ga-FAPI-46 PET/CT seems useful to improve detection of nodal metastasis in patients with CCs. Future studies should aim to compare [⁶⁸Ga]Ga-FAPI-46 PET/CT to surgical staging of pelvic and para-aortic LNs in patients with locally advanced CC.

Key Words: FAPI PET, cervical cancer, FDG PET, surgical lymph node staging

(*Clin Nucl Med* 2023;48: 150–155)

Globally, cervical cancer (CC) is the fourth most common cancer in women and ranks fourth in terms of mortality.¹ Cervical cancer usually spreads from regional to distant lymph nodes (LN) step-by-step: first to pelvic LNs and then para-aortic, mediastinal, and finally supraclavicular LN before manifesting in distant regions. Para-aortic and pelvic LN metastasis is the most important prognostic factor and plays a major role in treatment decision. Involvement of pelvic and para-aortic nodes should be assessed separately given the high impact on radiotherapy (RT) planning (ie, favoring extended-field RT in para-aortic spread).

Surgical laparoscopic staging allows exact tumor staging and treatment decision with a histopathological upstaging rate of 33% of all patients with CC, and it significantly improves the disease-free survival.^{2–5} Based on the randomized Uterus-11 study,⁵ the German S3 guideline for CC recommends laparoscopic staging for LN assessment in locally advanced CC.⁶ Non-invasive techniques to accurately stage cervical N-status still are an unmet need. Nevertheless, in many countries, [¹⁸F]F-FDG PET/CT is routinely used as a primary diagnostic tool for LN staging and RT planning.^{7–9} With a false-negative rate of up to 20%, accuracy of [¹⁸F]F-FDG PET/CT staging is inferior to operative nodal staging. This leads to growing interest in improving the accuracy of new tracers in PET/CT diagnostics.^{10,11}

Fibroblast activation protein inhibitor (FAPI) PET compounds allow detection of fibroblast activation protein (FAP), which is overexpressed by cancer-associated fibroblasts (CAFs) in the tumor microenvironment.¹² Just like FDG and FLT, the tracer is not cancer-specific. Given its novelty, reported clinical experience is

Received for publication September 21, 2022; revision accepted October 5, 2022.

From the *Department of Radiation Oncology, Cyberknife and Radiotherapy, University Hospital Cologne; †Department of Nuclear Medicine, Faculty of Medicine and University Hospital Cologne, University of Cologne; ‡Institute for Pathology, University Hospital of Cologne, Cologne; §German Center for Neurodegenerative Diseases (DZNE), Bonn-Cologne; ||Institute of Neuroscience and Medicine (INM-2), Molecular Organization of the Brain, Forschungszentrum Jülich; and ¶Department of Special Operative and Oncologic Gynecology, Asklepios-Clinic Hamburg-Altona, Asklepios Hospital Group, Hamburg, Germany.

Conflicts of interest and sources of funding: The authors have no conflicts of interest to declare. This study has been supported by SOFIE by the provision of precursors for FAPI synthesis. A.D. discloses research support from Siemens Healthineers, Life Molecular Imaging, GE Healthcare, AVID Radiopharmaceuticals, SOFIE and Eisai; Speaker Honorary and/or Advisory Boards fees from Siemens Healthineers, Sanofi, GE Healthcare, Biogen, Novo Nordisk; Invicro Stock from Siemens Healthineers, Lantheus Holding, and a patent pending for ¹⁸F-PSMA7 (PSMA PET imaging tracer).

All procedures performed in studies involving human participants were in accordance with the ethical standards of the institutional and/or national research committee and with the 1964 Helsinki Declaration and its later amendments or comparable ethical standards. Informed consent to undergo imaging and RT was obtained from all individual participants included in the study. The local institutional review board waived requirement to obtain consent for retrospective data analysis.

Authors Contributions: S.W., K.S.R., J.W., K.C., P.L., M.T., D.A.-B. and C.K. collected data. K.S.R., J.W., L.v.H., C.K. and A.D. interpreted imaging data. B.S.-M. performed histopathological analysis and staining. K.S. and T.F. supervised FAP synthesis and application and carefully read the manuscript. S.W., Chr.K. and S.M. interpreted data and drafted the manuscript. All authors carefully revised and approved the final version of the manuscript.

Correspondence to: Simone Wegen, MD, Department of Radiation Oncology, Cyberknife and Radiotherapy, University Hospital Cologne, Kerpener Str. 62, 50937 Cologne, Germany. E-mail: simone.wegen@uk-koeln.de.

Copyright © 2023 The Author(s). Published by Wolters Kluwer Health, Inc. This is an open-access article distributed under the terms of the Creative Commons Attribution-Non Commercial-No Derivatives License 4.0 (CCBY-NC-ND), where it is permissible to download and share the work provided it is properly cited. The work cannot be changed in any way or used commercially without permission from the journal.

ISSN: 0363-9762/23/4802-0150

DOI: 10.1097/RLU.00000000000004505

limited. We here report the first clinical data on the role of [⁶⁸Ga]Ga-FAPI-46-PET/CT for nodal staging of patients with proven CC.

METHODS

We retrospectively reviewed our clinical database for patients with histologically proven CC, who received [⁶⁸Ga]Ga-FAPI-46 PET/CT before surgical LN staging between March 2020 and April 2022. We found 7 women available for analysis. All patients received [⁶⁸Ga]Ga-FAPI-46 PET/CT scans for treatment planning. The scans were performed in RT positioning (arms up, full urinary bladder, small rectum volume). If available, [¹⁸F]F-FDG PET/CT scans and MRI were used for comparison. We performed histopathological LN correlation (FAPI/pathology) in 6 patients (all patients except patient 7; Table 1) and TBR measurements in 5 patients (all women except patients 3 and 7; Table 1).

All procedures were performed according to the regulations of the local authorities (District Administration of Cologne, Germany) and after the local institutional review board (University of Cologne) approved the retrospective analysis. This retrospective study was carried out in accordance with the Declaration of Helsinki, with the written consent of all patients to PET/CT imaging and inclusion of their data for scientific analysis.

PET/CT Imaging and Interpretation

Two independent reviewers evaluated all images, identified tumors and metastasis, and measured count rates (CRs) of tumor, metastasis, and reference tissue. In addition, the number of lesions and the number of LN metastasis were recorded and compared between both scans. A correlation of PET scan with CT scan was used to define tumor margins from bladder and to exclude unspecific findings. For simultaneous RT planning using the CT component, patients were instructed to not empty their bladder before PET/CT scans were performed (minimum requirement 200 mL).

Count rates were obtained from both scans drawing volumes of interests (VOIs) either in reference tissue (mediastinal blood pool and liver) or from primary tumors and nodal metastasis. The maximum and peak CRs (CR_{max} and CR_{peak}) were collected for tumors and metastatic tissue, whereas mean CRs (CR_{mean}) were measured for the reference tissue. CR_{max} and CR_{peak} were obtained by drawing a VOI around the malignant tissue; CR_{mean} values within reference tissues were measured within a spherical VOI of 2-cm diameter in the right liver lobe and within a spherical VOI of 1-cm diameter in the descending thoracic aorta representing the mediastinal blood pool. Tumor-to-background ratios (TBRs) of CR between suspicious lesions and reference tissue were measured from [¹⁸F]F-FDG PET/CT and [⁶⁸Ga]Ga-FAPI-46-PET/CT scans to measure

and quantify differences in accumulation of both tracers in primary tumor and metastasis.

One patient received an [¹⁸F]-FDG PET/CT and afterward a [⁶⁸Ga]Ga-FAPI-46-[¹⁸F]-FDG PET/CT (dual-tracer protocol) within one appointment.¹³ All other patients (n = 4) received PET/CT with [⁶⁸Ga]Ga-FAPI-46 and [¹⁸F]-FDG within 2 different appointments with a maximum time interval of 6 days between the 2 scans.

For [¹⁸F]-FDG PET/CT, a mean of 234 MBq (±37.8 MBq) [¹⁸F]-FDG was injected. Imaging was started approximately 71.5 minutes after IV injection (±17 minutes). [⁶⁸Ga]Ga-FAPI-46-PET/CT was performed approximately 50 minutes after IV injection (±23 minutes) with a mean of 152 MBq (±24 MBq) [⁶⁸Ga]Ga-FAPI-46.

Surgical Staging

After PET imaging, patients were referred to the department of gynecology and oncology to undergo laparoscopic staging before chemoradiation. The methodology of laparoscopic LN staging in CC has been described by other study groups⁵ and is part of the practical guideline of the European Society of Gynecological Oncology for management of patients with CC.^{5,14}

Surgical staging was performed via laparoscopy (transperitoneal/extraperitoneal access). Pelvic LN dissection has been performed in external iliac, obturatorial, and iliac common LNs, as well as in the para-aortic region up to the upper limit of renal vessels (comprehensive pelvic and para-aortic staging).

Histopathological Examination and FAP Staining

In histological-proven LN metastasis, immunohistochemistry (IHC) for FAP was performed on formalin-fixed paraffin-embedded tissue slides according to standard IHC protocols; 1- to 2-μm-thick tumor sections were stained for FAP (clone number ERP20021; Abcam) on Bond Max (Leica) stainer. Immunostaining was scored as previously described. Staining was designated as positive if cell surface staining on carcinoma-associated stromal cells was observed. Tumor-free LNs served as negative controls.

Statistical Analysis

Descriptive statistics were used to present patient characteristics and results. SPSS Statistics version 28 (IBM Corp, Armonk, NY) was used for statistical analysis. *P* ≤ 0.05 was considered to be statistically significant. To detect statistical differences, a Wilcoxon signed rank test for 2 continuous variables was performed.

RESULTS

Imaging data of 7 women were available for this study (Table 1 and Table 2). All patients had histologically confirmed CC before

TABLE 1. Patient Characteristics

Patient	Age, y	BMI, kg/m ²	ECOG	FIGO	TNM	HPV Status	Histology
1	35	20.7	0	IB	cT1b1 pN0 (0/37) cM0	Negative	Adeno
2	67	20.3	1	IIB	cT2b pn0 (0/16) cM0	Positive	Squamous
3*	67	34	1	IVA	cT4 pN0 (0/14) cM0	NA	Squamous
4	57	21.7	0	IIIB	cT1b1 pN1 (1/24) cM0	Positive	Squamous
5	56	19.5	0	IIIB	cT2 pn1 (2/11) cM0	NA	Adeno
6	34	18.30	0	IIIB	cT1b2 pN1a (2/50) cM0	Positive	Squamous
7†	46	19.4	0	IIIB	cT1b2 pN1 (14/39) cM0	Positive	Squamous

* Patient 3 has not been included in quantitative TBR analysis because of [⁶⁸Ga]Ga-FAPI-46 accumulation in the bladder (primary tumor in the cervix could not be defined).
†Patient 7 has not been included in quantitative TBR analysis and histopathological correlation because of long time delay (>3 months) and absence of [¹⁸F]F-FDG PET/CT scans (performed in another country).

BMI, body mass index; ECOG, Eastern Cooperative Oncology Group; FIGO, International Federation of Gynecology and Obstetrics; HPV, human papillomavirus; NA, not available.

TABLE 2. Site Involvement

Subject	FAPI Primary Tumor	Nodal Involvement According to							FAP IHC
		MRI	FDG Pelvine	FDG Para-aortic	FAPI Pelvine	FAPI Para-aortal	Patho Pelvine	Patho Para-aortic	
1	Positive	No	No	No	No	No	No	No	No
2	Positive	No	No	No	No	No	No	No	No
3	Positive	No	No	No	No	No	No	No	No
4	Positive	Yes	Yes (2)	No	Yes (2)	No	Yes (1/24)	No	Yes
5	Positive	NA	No	No	Yes (2)	No	Yes (2/11)	No	Yes
6	Weak positive	No	No	No	No	No	Yes (1/9)	No	(Yes)
7	Positive	NA	Na	Na	Yes (>2)	Yes (>5)	Yes (5/15)	Yes (9/24)	Yes
Comparison of FAPI positivity, FDG positivity, MRI positivity, and histopathological positivity of pelvic and para-aortic lymph nodes in 7 women with proven cervical cancer. NA, not available.									

imaging and had been referred for primary chemoradiation. One patient with a T4a tumor stage has developed a vesicovaginal fistula before chemoradiation (but following surgical staging); thus, an anterior exenteration was performed before adjuvant chemoradiation. Five of 7 patients (71.4%) proved to have squamous cell carcinoma. Six of 7 women received [¹⁸F]F-FDG PET/CT and [⁶⁸Ga]Ga-FAPI-46 PET/CT with a maximum time interval of 3 weeks before surgical staging. One woman (patient 3; Table 1) had a primary tumor (CC) indistinguishable from bladder uptake in both PET scans. This patient was excluded from TBR analysis. Another patient (patient 7; Table 1) was excluded from the histopathological correlation because she received her [¹⁸F]-FDG PET/CT in a different country 3 months before she received [⁶⁸Ga]Ga-FAPI-46-PET/CT in our clinic (no comparison between the scans because of long time interval).

- Three patients (patients 1–3) had node-negative PET scans ([¹⁸F]-FDG PET/CT and [⁶⁸Ga]Ga-FAPI-46-PET/CT) and no metastatic LNs in the histopathology (true negative for [¹⁸F]-FDG PET/CT and [⁶⁸Ga]Ga-FAPI-46-PET/CT).
- One woman (patient 4) had 2 metastatic pelvic LNs in both [¹⁸F]-FDG PET/CT and [⁶⁸Ga]Ga-FAPI-46-PET/CT scans (same localization), of which one proved to be metastatic afterward in histopathology (true positive for [¹⁸F]-FDG PET/CT and [⁶⁸Ga]Ga-FAPI-46-PET/CT).

- One woman (patient 5) had a negative [¹⁸F]F-FDG PET/CT scan but 2 FAPI-positive pelvic LNs (both sides of the pelvis), which proved to be metastatic in the histopathological examination (true positive for [⁶⁸Ga]Ga-FAPI-46 PET/CT, false negative for [¹⁸F]F-FDG PET/CT). [⁶⁸Ga]Ga-FAPI-46 PET/CT and [¹⁸F]F-FDG PET/CT images of 1 pelvic LN are demonstrated in Figure 1.
- One woman (patient 6) had negative scans ([¹⁸F]F-FDG PET/CT and [⁶⁸Ga]Ga-FAPI-46 PET/CT) but proved to have 1 small (3 mm) pelvic nodal metastasis (micrometastasis, false negative for [¹⁸F]F-FDG PET/CT and [⁶⁸Ga]Ga-FAPI-46 PET/CT).
- One woman (patient 7) had her [¹⁸F]F-FDG PET/CT scan 3 months earlier than the [⁶⁸Ga]Ga-FAPI-46 PET/CT and in a different country. We accessed these scans and medical reports (pelvic positive LNs) but decided not to compare these FDG scans to the FAP scans because of large interval between the scans. In [⁶⁸Ga]Ga-FAPI-46 PET/CT, she had vast nodal metastasis in both pelvis and the para-aortic region. In surgical staging, the patient had 5/15 metastatic pelvic LNs and 9/24 metastatic para-aortic LNs (true positive for [⁶⁸Ga]Ga-FAPI-46 PET/CT; Fig. 2).

Metastatic lesions were stained for FAP using IHC. Here, all metastases with focal FAP uptake in [⁶⁸Ga]Ga-FAPI-46 PET/CT were strongly positive for FAP by IHC (3/7 patients). One patient

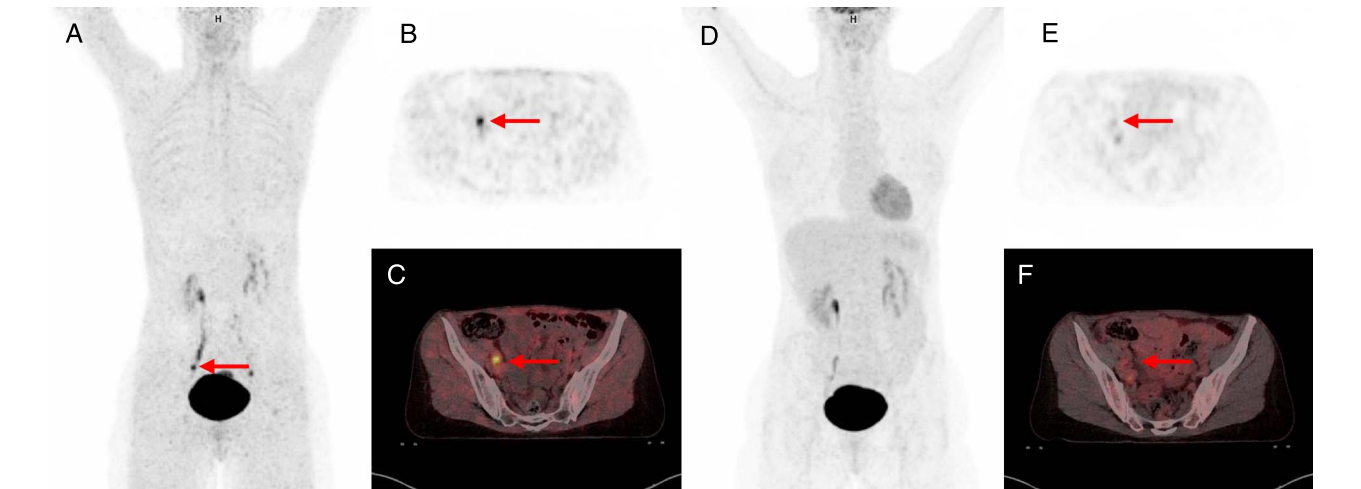


FIGURE 1. Suspicious pelvic LN in a 56-year old woman (patient 5; Table 1) with metastatic CC [⁶⁸Ga]Ga-FAPI-46 PET/CT (A–C) and [¹⁸F]F-FDG PET/CT (D–F). A, MIP of [⁶⁸Ga]Ga-FAPI-46 PET/CT, red arrow indicating LN metastasis. B, MIP axial, red arrow indicating LN metastasis. C, FAP uptake in LN metastasis in the right pelvis. D, MIP of [¹⁸F]F-FDG PET/CT. E, MIP (axial) of [¹⁸F]F-FDG PET/CT. F, No FDG uptake in pelvic LNs. The pathological examination confirmed metastasis in that LN. There was no correlation in the FDG scan.

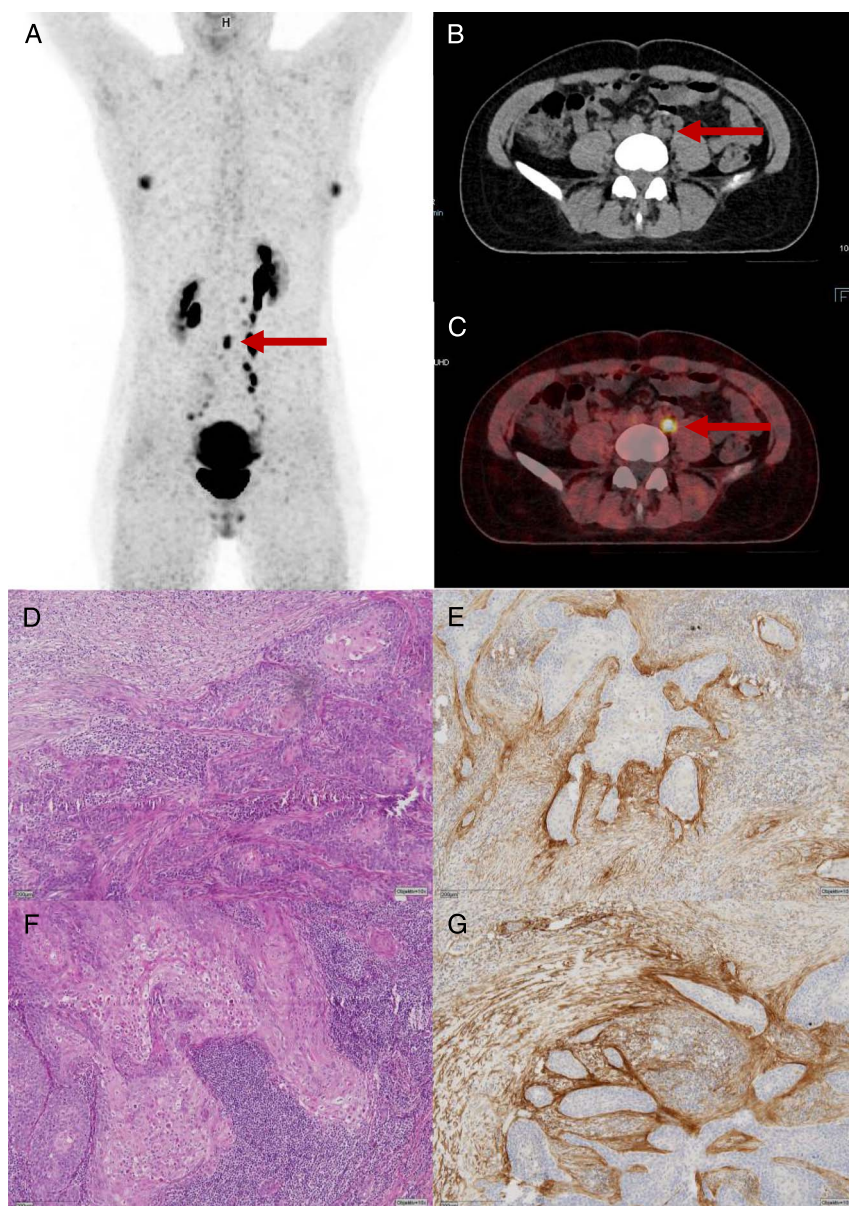


FIGURE 2. [^{68}Ga]Ga-FAPI-46 PET/CT scans and histology of a 46-year-old woman with metastatic CC (patient 7; Table 1). **A**, MIP with nodal metastasis in the pelvic and para-aortic region, red arrow indicating a left iliac LN. **B**, CT scan (axial) with left iliac LN (CT-correlate, red arrow). **C**, FAP uptake in the same left iliac LN. **D + F**, Hematoxylin-eosin staining of metastatic pelvic LN. **E + G**, Positive FAP staining of metastatic LN.

(patient 6) with micrometastasis in a pelvic LN (FDG and FAP negative) showed only a very slight FAP staining in the IHC. An example of LN metastasis with a strongly positive FAP staining (patient 7) is presented in Figure 2.

Tumor-to-Background Ratios

In our cohort, 4 of 5 patients received their PET scans on 2 different days, whereas 1 patient received them in the same way (dual-tracer protocol).¹³ Overall, [^{68}Ga]Ga-FAPI-46 PET/CT showed better TBRs in both primary tumor and nodal metastasis. Values for TBR_{max} liver (CR_{max} primary tumor/ CR_{mean} liver) were 32.02 (median; range, 12.5–61.56) for [^{68}Ga]Ga-FAPI-46 PET/CT versus 5.15 (median; range, 3.68–14.16) for [^{18}F]F-FDG PET/CT. Median TBR_{max} blood pool (CR_{max} primary tumor/ CR_{mean} blood pool) was 18.45 ([^{68}Ga]

Ga-FAPI-46 PET/CT; range, 13.17–24.25) versus 6.85 (FDG; range, 4.86–19.11). In nodal metastasis, [^{68}Ga]Ga-FAPI-46 PET/CT showed a higher TBR compared with [^{18}F]F-FDG PET/CT: median TBR_{max} liver (CR_{max} metastasis/ CR_{mean} liver) was 14.55 (range, 12.71–23.1) versus 1.39 (range, 1.3–3.41), median TBR_{max} blood pool (CR_{max} metastasis/ CR_{mean} blood pool) was 7.97 ([^{68}Ga]Ga-FAPI-46 PET/CT; range, 6.46–13.82) versus 1.8 ([^{18}F]F-FDG PET/CT; range, 1.69–4.37). Table 3 and Figure 3 show TBR measurements for [^{68}Ga]Ga-FAPI-46 PET/CT and [^{18}F]F-FDG PET/CT for primary tumor and nodal metastasis (TBR_{max} and TBR_{peak} values).

DISCUSSION

To our best knowledge, this is the first clinical study about use of [^{68}Ga]Ga-FAPI-46 PET/CT in patients with locally advanced

TABLE 3. Tumor-to-Background Ratios for [¹⁸F]F-FDG PET/CT and [⁶⁸Ga]Ga-FAPI-46 PET/CT

Site	Background	Tracer	TBR _{max} Median (Range)	TBR _{peak} Median (Range)
Primary tumor	Blood pool	FDG	6.85 (4.86–19.11)	6.42 (4.19–19.24)
		FAPI	18.45 (13.17–24.25)	16.85 (12.11–27.42)
	Liver	FDG	5.15 (3.68–14.16)	4.64 (3.66–14.16)
		FAPI	32.02 (12.5–61.56)	31.18 (12.5–51.83)
Metastasis	Blood pool	FDG	1.8 (1.69–4.37)	1.39 (1.36–1.45)
		FAPI	7.97 (6.46–13.82)	4.8 (4.2–6.55)
	Liver	FDG	1.39 (1.3–3.41)	1.08 (1.06–1.11)
		FAPI	14.55 (12.71–23.1)	8.91 (7.94–10.94)

CC. [⁶⁸Ga]Ga-FAPI-46 PET/CT in CC has promising features and may be more accurate than [¹⁸F]F-FDG PET/CT for nodal staging. In addition, we found a favorable TBR, which matches reported data in gynecological tumors and nodal metastasis.^{15,16} For nodal staging purposes of CC, CT, MRI, and [¹⁸F]F-FDG PET/CT do not show sufficient accuracy.^{17–19} Despite improved image resolution and tracers, there is still a high rate of false-negative findings compared with surgical staging facing severe consequences for patients when false treatment decisions are made. The use of [¹⁸F]F-FDG PET/CT is increasing in the field of CC, partly because of growing evidence in other malignancies during the last years (eg, in lung malignancies, head and neck cancer, sarcoma) and better availability globally, partly because it is more convenient for patients than surgical staging (no

anesthesia and no preoperative preparations—some patients reject surgical staging for these reasons). In our society, we are facing a growing number of old patients with secondary diseases, mainly metabolic syndrome (obesity). Here, surgical staging bears a certain risk, and it could be great offering these patients PET staging as a solid alternative. We faced difficulties in defining the local CC tumor volume, as [⁶⁸Ga]Ga-FAPI-46 accumulation in the normal endometrium seems to be cycle dependent.²⁰ In addition, for dose-planning purposes, patients had to meet some criteria regarding rectal filling (as empty as possible) and a bladder volume of at least 200 mL. This resulted in tracer accumulation in the bladder and impeded the demarcation of the actual tumor volume in the cervix, although proper detection of the primary tumor was possible in 6 of 7 patients.

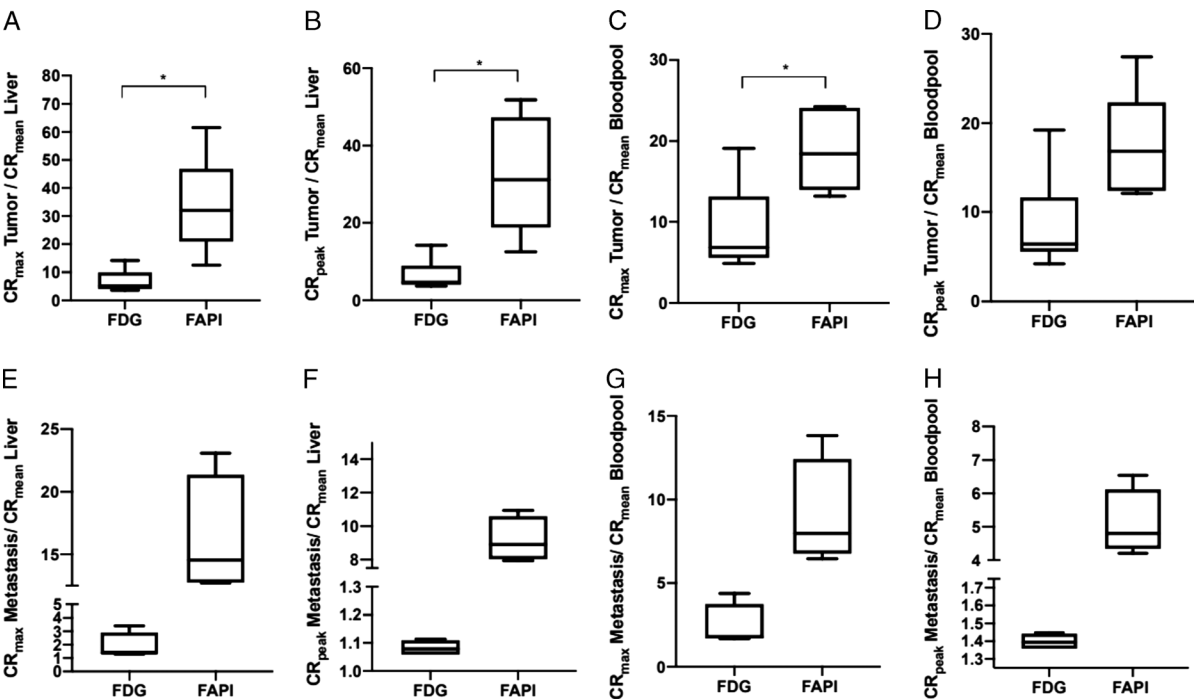


FIGURE 3. Tumor-to-background ratios. A, TBR_{max} liver (tumor). B, TBR_{peak} liver (tumor). C, TBR_{max} blood pool (tumor). D, TBR_{peak} blood pool (tumor). E, TBR_{max} liver (metastasis). F, TBR_{peak} liver (metastasis). G, TBR_{max} blood pool (metastasis). H, TBR_{peak} blood pool (metastasis). TBR was calculated by dividing CR_{max} or CR_{peak} (tumor or metastasis) by CR_{mean} (liver or blood pool): TBR_{max} liver (tumor) = CR_{max} tumor/CR_{mean} liver, TBR_{peak} liver (tumor) = CR_{peak} tumor/CR_{mean} liver, TBR_{max} blood pool (tumor) = CR_{max} tumor/CR_{mean} blood pool, TBR_{peak} blood pool (tumor) = CR_{peak} tumor/CR_{mean} blood pool, TBR_{max} liver (metastasis) = CR_{max} metastasis/CR_{mean} liver, TBR_{peak} liver (metastasis) = CR_{peak} metastasis/CR_{mean} liver, TBR_{max} blood pool (metastasis) = CR_{max} metastasis/CR_{mean} blood pool, TBR_{peak} blood pool (metastasis) = CR_{peak} metastasis/CR_{mean} blood pool. Of note: [¹⁸F]F-FDG PET/CT of patient 7 was not available. Primary tumor of patient 3 was not measurable given the high bladder uptake. *0.05 > P > 0.01.

In our cohort, 1 patient had histologically proven pelvic nodal metastasis smaller than 3 mm and with low density of FAP, as identified in IHC. This node was missed by both [^{18}F]F-FDG PET/CT and [^{68}Ga]Ga-FAPI-46 PET/CT. Micrometastatic disease and low FAP expression may be potential pitfalls for [^{68}Ga]Ga-FAPI-46 PET/CT and are important to consider in future diagnostic trials.

Insufficient radiation dose and growing radiation resistance of tumor cells are major reasons for tumor recurrence after RT. The role of CAFs in the tumor microenvironment and radiation resistance is still not entirely understood. There is some evidence that they can promote tumor progression and invasiveness as well as boosting antitumorigenic effects. The effect of radiation on CAFs alters their tumor-promoting capability, but unfortunately, treated CAFs show both enhancing and diminishing protumorigenic potential. For nasopharyngeal cancer, a Chinese study generated first evidence that CAFs can promote the survival of irradiated NPC cells via the nuclear factor- κB pathway and induce radioresistance.²¹ Reducing the survival of CAF-induced tumor cells with CAF inhibitors or FAP-targeted therapies may counteract this mechanism, but clinical data are still lacking.^{21,22}

At present, special caution is required when upstaging a patient based on [^{68}Ga]Ga-FAPI-46 PET/CT alone. [^{68}Ga]Ga-FAPI-46 uptake has been described in various conditions such as benign tumors, inflammation, degenerative diseases, fibrosis, and granulomatosis. The knowledge and interpretation of these pitfalls are important in the management of incidental findings in patients referred for cancer staging indications. Recent studies suggest that image acquisition earlier than 60 minutes or even multiple-minute time points improve the discrimination of malignant lesions.^{23,24}

The strength of the reported study is the 1:1 correlation of localization and histological confirmation of suspicious LNs by performing laparoscopic nodal staging after [^{68}Ga]Ga-FAPI-46 PET/CT and [^{18}F]F-FDG PET/CT. This study benefits from the fact that patients were in RT positioning, and immobilization devices were used for all imaging data (better comparability of both scans). Also, our patients had no prior treatment, which could have distorted imaging quality. Main drawbacks are its small sample size and retrospective nature with inherent bias. The study acts as a proof of principle for further investigation. To avoid time delay in starting chemoradiation, a coregistration of [^{68}Ga]Ga-FAPI-46 and [^{18}F]F-FDG has been established (dual-tracer PET/CT protocol¹³) and already been performed in 1 patient of this cohort. Further studies are therefore needed to determine the value of [^{68}Ga]Ga-FAPI-46 PET/CT for noninvasive nodal staging of CC compared with surgical staging.

CONCLUSIONS

In a cohort of 7 women, we find better nodal tumor detection for [^{68}Ga]Ga-FAPI-46 PET/CT compared with [^{18}F]F-FDG PET/CT. All [^{68}Ga]Ga-FAPI-46–positive nodal metastases were confirmed by histopathology with a strong FAP expression in IHC. Our results call for trials determining the diagnostic value of [^{68}Ga]Ga-FAPI-46 PET/CT in primary staging of CC.

REFERENCES

- Bray F, Ferlay J, Soerjomataram I, et al. Global cancer statistics 2018: GLOBOCAN estimates of incidence and mortality worldwide for 36 cancers in 185 countries. *CA Cancer J Clin*. 2018;68:394–424.
- Marnitz S, Martus P, Köhler C, et al. Role of surgical versus clinical staging in chemoradiated FIGO stage IIB–IVA cervical cancer patients—acute toxicity and treatment quality of the Uterus-11 multicenter phase III intergroup

trial of the German Radiation Oncology Group and the Gynecologic Cancer Group. *Int J Radiat Oncol Biol Phys*. 2016;94:243–253.

- Marnitz S, Köhler C, Roth C, et al. Stage-adjusted chemoradiation in cervical cancer after transperitoneal laparoscopic staging. *Strahlenther Onkol*. 2007;183:473–478.
- Tsunoda AT, Marnitz S, Soares Nunes J, et al. Incidence of histologically proven pelvic and para-aortic lymph node metastases and rate of upstaging in patients with locally advanced cervical cancer: results of a prospective randomized trial. *Oncology*. 2017;92:213–220.
- Marnitz S, Tsunoda AT, Martus P, et al. Surgical versus clinical staging prior to primary chemoradiation in patients with cervical cancer FIGO stages IIB–IVA: oncologic results of a prospective randomized international multicenter (Uterus-11) intergroup study. *Int J Gynecol Cancer*. 2020;30:1855–1861.
- S3-Leitlinie Diagnostik TuNDPmZ. AWMF-Registernummer 032/033OL. Available at: www.awmf.de. Accessed October 31, 2019.
- Hansen H, Loft A, Berthelsen A, et al. Introducing PET/CT in cervical cancer staging procedures leads to stage migration and selection bias. *Int J Radiat Oncol*. 2014;90:S481–S482.
- Grueneisen J, Schaarschmidt BM, Heubner M, et al. Integrated PET/MRI for whole-body staging of patients with primary cervical cancer: preliminary results. *Eur J Nucl Med Mol Imaging*. 2015;42:1814–1824.
- Adam JA, Arkies H, Hinnen K, et al. ^{18}F -FDG-PET/CT guided external beam radiotherapy volumes in inoperable uterine cervical cancer. *Q J Nucl Med Mol Imaging*. 2018;62:420–428.
- Frumovitz M, Ramirez PT, Macapinlac HA, et al. Anatomic location of PET-positive aortocaval nodes in patients with locally advanced cervical cancer implications for surgical staging. *Int J Gynecol Cancer*. 2012;22:1203–1207.
- Gouy S, Seebacher V, Chargari C, et al. False negative rate at (^{18}F)F-FDG PET/CT in para-aortic lymphnode involvement in patients with locally advanced cervical cancer: impact of PET technology. *BMC Cancer*. 2021;21:135.
- Kratochwil C, Flechsig P, Lindner T, et al. (^{68}Ga)Ga-FAPI PET/CT: tracer uptake in 28 different kinds of cancer. *J Nucl Med*. 2019;60:801–805.
- Roth KS, Voltin CA, van Heek L, et al. Dual-tracer PET/CT protocol with [^{18}F]FDG and [^{68}Ga]Ga-FAPI-46 for cancer imaging: a proof of concept. *J Nucl Med*. 2022;63:1683–1686.
- Cibula D, Potter R, Planchamp F, et al. The European Society of Gynaecological Oncology/European Society for Radiotherapy and Oncology/European Society of Pathology guidelines for the management of patients with cervical cancer. *Radiother Oncol*. 2018;127:404–416.
- Giesel FL, Kratochwil C, Lindner T, et al. (^{68}Ga)Ga-FAPI PET/CT: biodistribution and preliminary dosimetry estimate of 2 DOTA-containing FAP-targeting agents in patients with various cancers. *J Nucl Med*. 2019;60:386–392.
- Dendl K, Koerber SA, Finck R, et al. ^{68}Ga -FAPI-PET/CT in patients with various gynecological malignancies. *Eur J Nucl Med Mol Imaging*. 2021;48:4089–4100.
- Boughanim M, Leboulleux S, Rey A, et al. Histologic results of para-aortic lymphadenectomy in patients treated for stage IB2/II cervical cancer with negative [^{18}F]fluorodeoxyglucose positron emission tomography scans in the para-aortic area. *J Clin Oncol*. 2008;26:2558–2561.
- Grigsby PW, Singh AK, Siegel BA, et al. Lymph node control in cervical cancer. *Int J Radiat Oncol Biol Phys*. 2004;59:706–712.
- Scheidler J, Hricak H, Yu KK, et al. Radiological evaluation of lymph node metastases in patients with cervical cancer. A meta-analysis. *JAMA*. 1997;278:1096–1101.
- Zhang X, Song W, Qin C, et al. Uterine uptake of ^{68}Ga -FAPI-04 in uterine pathology and physiology. *Clin Nucl Med*. 2022;47:7–13.
- Huang W, Zhang L, Yang M, et al. Cancer-associated fibroblasts promote the survival of irradiated nasopharyngeal carcinoma cells via the NF- κB pathway. *J Exp Clin Cancer Res*. 2021;40:87.
- Ferdinandus J, Costa PF, Kessler L, et al. Initial clinical experience with (90)Y-FAPI-46 radioligand therapy for advanced-stage solid tumors: a case series of 9 patients. *J Nucl Med*. 2022;63:727–734.
- Glatting FM, Hoppner J, Liew DP, et al. Repetitive early FAPI-PET acquisition comparing FAPI-02, FAPI-46 and FAPI-74: methodological and diagnostic implications for malignant, inflammatory and degenerative lesions. *J Nucl Med*. 2022.
- Ferdinandus J, Kessler L, Hirma N, et al. Equivalent tumor detection for early and late FAPI-46 PET acquisition. *Eur J Nucl Med Mol Imaging*. 2021;48:3221–3227.